# Global energy-preserving local mesh-refined S-FDTD schemes for two dimensional Maxwell's equations in Drude metamaterials

Dong Liang[a,*], Cong Wang[a]

[a] *Department of Mathematics and Statistics, York University, Toronto, Ontario, M3J 1P3, Canada*

**Abstract**

Modelling electromagnetic propagation in metamaterials is of importance in many applications. Designing efficient local mesh refinements is crucial to improve the resolution capacity of solution for solving Maxwell's equations within metamaterials and it is a difficult task to develop local mesh-refined schemes for preserving global energy across the interfaces between coarse and fine meshes. In this paper, we develop two global energy-preserving local mesh-refined splitting FDTD schemes for Maxwell's equations with Drude model. By combining with the energy-conserved splitting FDTD methods, the local mesh-refined interface schemes are established on the interfaces of coarse and fine meshes, which ensure global energy preserving. We prove that the developed GEP-LMR-S-FDTD schemes satisfy global energy conservation and are unconditionally stable. Meanwhile, fast implementation of the GEP-LMR-S-FDTD schemes is investigated to compute the metamaterial elctromagnetic problems. Numerical experiments show the excellent performance of the schemes.

*Keywords:* Electromagnetic Drude system, Energy-preserving S-FDTD, Local mesh refinement, Global energy conservation, Unconditional stability,

## 1. Introduction

Since the advance of small metallic wires and split-ring resonators in 2001, there has been a dramatic research interest of metamaterials and applications such as radar, microwave, optical components and invisible cloak design [1, 2, 3, 4], etc. Modelling electromagnetic propagation in metamaterials has been playing an important role in its development and application. Methods have been developed for solving Maxwell's equations with dispersive media such as FDTDs in [5, 6, 7, 8, 9] and FEMs [10, 11, 12, 13, 14], etc. Due to the metamaterial's microscale and local geometric structure and the local solution behavior, numerical technique is required to improve the resolution capacity of solution. In the presence of different mesh scales, the sudden change of mesh sizes inevitably produces spurious reflections in numerical waves. Designing efficient local mesh refinements over grids is crucial for solving Maxwell's equations within metamaterials.

Finite-difference time-domain (FDTD) method [15] is a widely used numerical method to solve the Maxwell's equations because of its simplicity and flexibility [16]. With the realization of metamaterials, FDTD schemes have been applied to solve the electromagnetic models in metamaterials [5, 7, 17, 18]. For improving the stability, ADI-FDTD schemes

*Corresponding author.
*Email addresses:* dliang@yorku.ca (Dong Liang), cwang422@yorku.ca (Cong Wang)

[19, 20] and LOC-FDTD schemes [21, 22] were further developed. Recently, EC-S-FDTD schemes [23, 24] were developed for preserving global energy and stability in solutions to Maxwell's equation in metamaterials.

Efforts on the local mesh refinement strategies to FDTD schemes have been made for solving classical Maxwell's equations. Kim and Hoefer [25] proposed a local time and space mesh refinement algorithm based on interpolation at the interface of coarse and fine meshes. Zakharian et al. [26] studied a second-order accurate local time and space mesh refinement algorithm from high-order interpolation at the coarse and fine grid interfaces. Chen and Ahmed [27] proposed a hybrid ADI-FDTD locally graded algorithm. Collino et al. [28, 29] developed a space-time mesh refinement algorithm leading to a discrete "modified" energy identity through two various discretization meshes. However, these mesh refinement methods may suffer from severe CFL condition of stability and do not satisfy energy conservation. Recently, energy-preserving local mesh-refined S-FDTD schemes [30] were developed for solving two-dimensional Maxwell's equations by the local mesh refinements, which ensure energy conservation while keeping spatial accuracy and avoiding oscillations. However, there were no work on local mesh refinements for metamaterial Maxwell's equations. It is an important and difficult task to develop local mesh refinements for Maxwell's equations in metamaterials for preserving global energy across the interfaces between coarse and fine meshes.

In this paper, we develop two global energy-preserving local mesh-refined splitting FDTD schemes, i.e. GEP-LMR-S-FDTD-I and GEP-LMR-S-FDTD-II, for solving two dimensional Maxwell's equations within Drude meta-materials over local refinements. The electromagnetic Drude model is to describe the resonance of nuclei-bounded electrons in dielectrics by the damped oscillation with a restoring force in metamaterials. In addition to electric and magnetic fields, induced electric and magnetic currents are produced in metamaterials. The global energy of electromagnetic waves in the metamaterials remains unchanged, which contains the electric and magnetic energy, the induced electric and magnetic current energy and the accumulated heat energy transferred from the induced electromagnetic energy during the polarization process in [32, 23]. To design the local refinements, it is significant to keep the inherent conservative properties of the original electromagnetic propagation across the interfaces between coarse mesh and fine mesh. By combining with the energy-conserved splitting FDTD methods, the local mesh refined interface schemes are established on the interfaces of coarse and fine meshes for Maxwell's equations within Drude meta-materials, which ensure global energy preserving. Two schemes, GEP-LMR-S-FDTD-I and GEP-LMR-S-FDTD-II, are developed for solving Maxwell's equations in Drude metamaterials, where GEP-LMR-S-FDTD-I is first order in time and second-order in space while GEP-LMR-S-FDTD-II is second order in both time and space. We prove that both schemes satisfy global energy conservation and are unconditionally stable. Meanwhile, the fast implementation of GEP-LMR- S-FDTD schemes is investigated to compute the metamaterial electromagnetic problems. At each stage, we transform the coupled system into (1) first solving the coarse mesh unknowns of electric field and the averages of fine mesh unknowns of electric field on line structures and (2) then solving the fine mesh unknowns of electric field and interface coarse unknowns of electric field on "inverted U" structures. These lead to two different kind tridiagonal systems and can be efficiently solved. The numerical experiments are conducted and show the excellent performance of the GEP-LMR-S-FDTD schemes.

The rest of paper is organized as follows. In Section 2, we describe Maxwell's equations

within Drude meta-materials in two dimensions and some notations. Section 3 discusses the development of the GEP-LMR-S-FDTD-I scheme and its fast implementation. Section4 describes the EP-LMR-S-FDTD-II scheme. In Section 5, we prove the schemes global energy preserving and unconditionally stable. Numerical experiments are given and analyzed in Section 6.

## 2. Model of electromagnetic propagation in metamaterials and some notations

### *2.1. Maxwell's equations with Drude model*

The electromagnetic propagation in metamaterials is described by the Maxwell's equations

$$\frac{\partial \mathbf{D}}{\partial t} = \nabla \times \mathbf{H}, \tag{1}$$

$$\frac{\partial \mathbf{B}}{\partial t} = -\nabla \times \mathbf{E}, \tag{2}$$

where $\mathbf{E}(\mathbf{x}, t)$ and $\mathbf{H}(\mathbf{x}, t)$ are the electric and magnetic fields, $\mathbf{D}(\mathbf{x}, t)$ and $\mathbf{B}(\mathbf{x}, t)$ are the electric displacement and the magnetic flux density, respectively. They are related by the constitutive relationships:

$$\mathbf{D} = \epsilon_0 \mathbf{E} + \mathbf{P}, \ \mathbf{B} = \mu_0 \mathbf{H} + \mathbf{M}, \tag{3}$$

where $\epsilon_0$ is the vacuum permittivity, $\mu_0$ is the vacuum permeability, and $\mathbf{P}$ and $\mathbf{M}$ are the induced electric and magnetic polarizations.

The Drude model of $\mathbf{P}$ and $\mathbf{M}$ is to describe the resonance of nuclei-bounded electrons in dielectrics by the damped oscillation with a restoring force in metamaterials [31]. Let $\mathbf{r}$ be the collection of damped and noninteracting electrons of displacement, $m$ and $q$ represent the mass and effective charge respectively. Under the action of electric filed, the equation of motion [24, 32, 33, 34] is

$$q\mathbf{E} = m(\frac{\partial^2 \mathbf{r}}{\partial t^2} + \Gamma_e \frac{\partial \mathbf{r}}{\partial t}) \tag{4}$$

where $\Gamma_e$ is the electric damping frequency. Let $N$ be number of electrons and $\mathbf{P}$ is polarization, then

$$\mathbf{P} = Nq\mathbf{r} \tag{5}$$

Then, the relation between $\mathbf{P}$ and $\mathbf{E}$ can be expressed as

$$\frac{\partial^2 \mathbf{P}}{\partial t^2} + \Gamma_e \frac{\partial \mathbf{P}}{\partial t} = \epsilon_0 \omega_{pe}^2 \mathbf{E} \tag{6}$$

where $\omega_{pe} = (\frac{Nq^2}{m\epsilon_0})^{\frac{1}{2}}$ is the plasma frequency. Similarly,

$$\frac{\partial^2 \mathbf{M}}{\partial t^2} + \Gamma_m \frac{\partial \mathbf{M}}{\partial t} = \mu_0 \omega_{pm}^2 \mathbf{H}, \tag{7}$$

where $\Gamma_m$ is the magnetic damping frequency and $\omega_{pm} = (\frac{Nq^2}{m\mu_0})^{\frac{1}{2}}$ is the magnetic plasma frequency. Introduce the induced electric current $\mathbf{J}$ and the induced magnetic density $\mathbf{K}$ as

$$\mathbf{J} = \frac{\partial \mathbf{P}}{\partial t}, \quad \mathbf{K} = \frac{\partial \mathbf{M}}{\partial t}. \tag{8}$$

Hence, the Maxwell's equations with Drude model can be described as

$$\epsilon_0 \frac{\partial \mathbf{E}}{\partial t} = \nabla \times \mathbf{H} - \mathbf{J} \tag{9}$$

$$\mu_0 \frac{\partial \mathbf{H}}{\partial t} = -\nabla \times \mathbf{E} - \mathbf{K} \tag{10}$$

$$\frac{1}{\epsilon_0 \omega_{pe}^2} \frac{\partial \mathbf{J}}{\partial t} + \frac{\Gamma_e}{\epsilon_0 \omega_{pe}^2} \mathbf{J} = \mathbf{E} \tag{11}$$

$$\frac{1}{\mu_0 \omega_{pm}^2} \frac{\partial \mathbf{K}}{\partial t} + \frac{\Gamma_m}{\mu_0 \omega_{pm}^2} \mathbf{K} = \mathbf{H} \tag{12}$$

for $(\mathbf{x}, t) \in \Omega \times (0, T]$. We consider the perfect electric conduct (PEC) condition

$$\mathbf{n} \times \mathbf{E} = \mathbf{0}, \quad \text{on} \quad \partial\Omega \tag{13}$$

and the initial conditions

$$\mathbf{E}(\mathbf{x}, 0) = \mathbf{E}_0(\mathbf{x}), \ \mathbf{H}(\mathbf{x}, 0) = \mathbf{H}_0(\mathbf{x}), \tag{14}$$

$$\mathbf{J}(\mathbf{x}, 0) = \mathbf{J}_0(\mathbf{x}), \ \mathbf{K}(\mathbf{x}, 0) = \mathbf{K}_0(\mathbf{x}). \tag{15}$$

We consider the TE model of Maxwell's equations with Drude model in two dimensions:

$$\epsilon_0 \frac{\partial E_x}{\partial t} = \frac{\partial H_z}{\partial y} - J_x \tag{16}$$

$$\epsilon_0 \frac{\partial E_y}{\partial t} = -\frac{\partial H_z}{\partial x} - J_y \tag{17}$$

$$\mu_0 \frac{\partial H_z}{\partial t} = \frac{\partial E_x}{\partial y} - \frac{\partial E_y}{\partial x} - K_z \tag{18}$$

$$\gamma_e \frac{\partial J_x}{\partial t} + \gamma_e \Gamma_e J_x = E_x \tag{19}$$

$$\gamma_e \frac{\partial J_y}{\partial t} + \gamma_e \Gamma_e J_y = E_y \tag{20}$$

$$\gamma_m \frac{\partial K_z}{\partial t} + \gamma_m \Gamma_m K_z = H_z \tag{21}$$

for $(x, y) \in \Omega = [a, b] \times [c, d]$, $t \in (0, T]$, where $\gamma_e = (\epsilon_0 \omega_{pe}^2)^{-1}$ and $\gamma_m = (\mu_0 \omega_{pm}^2)^{-1}$. PEC boundary condition is provided

$$E_x(x, c, t) = E_x(x, d, t) = 0, \ E_y(a, y, t) = E_y(b, y, t) = 0, \tag{22}$$

and the initial conditions are

$$E_x(x, y, 0) = E_{x_0}(x, y), \ E_y(x, y, 0) = E_{y_0}(x, y), \ H_z(x, y, 0) = H_{z_0}(x, y), \tag{23}$$

$$J_x(x, y, 0) = J_{x_0}(x, y), \ J_y(x, y, 0) = J_{y_0}(x, y), \ K_z(x, y, 0) = K_{z_0}(x, y). \tag{24}$$

In the metamaterials, the global energy of electromagnetic wave of problem (16) - (24) remains unchanged, i.e. the global energy is conserved for any time $t > 0$, as

$$\begin{aligned}
&\frac{1}{2}\int_\Omega \{\epsilon_0[E_x(t)^2 + E_y(t)^2] + \mu_0[H_z(t)^2] + \gamma_e[J_x(t)^2 + J_y(t)^2] + \gamma_m[K_z(t)^2]\}dxdy \\
&\quad + \int_0^t \int_\Omega \{\gamma_e\Gamma_e[J_x(\tau)^2 + J_y(\tau)^2] + \gamma_m\Gamma_m[K_z(\tau)^2]\}dxdyd\tau \qquad (25)\\
&= \frac{1}{2}\int_\Omega \{\epsilon_0[E_x(0)^2 + E_y(0)^2] + \mu_0[H_z(0)^2] + \gamma_e[J_x(0)^2 + J_y(0)^2] + \gamma_m[K_z(0)^2]\}dxdy.
\end{aligned}$$

The global energy includes the electric and magnetic energy, induced electric and magnetic current energy and the accumulated memory of the induced electric and magnetic current energy in metamaterials during the propagation.

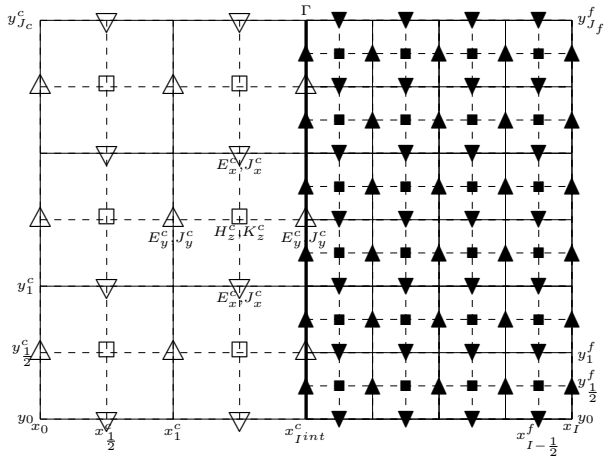


Figure 1: Sub-domain refinement of staggered mesh: □ for $H^c_{z_{i+\frac{1}{2},j+\frac{1}{2}}}$ and $K^c_{z_{i+\frac{1}{2},j+\frac{1}{2}}}$, △ for $E^c_{y_{i,j+\frac{1}{2}}}$ and $J^c_{y_{i,j+\frac{1}{2}}}$, ▽ for $E^c_{x_{i+\frac{1}{2},j}}$ and $J^c_{x_{i+\frac{1}{2},j}}$ and ■ for $H^f_{z_{i+\frac{1}{2},j+\frac{1}{2}}}$ and $K^f_{z_{i+\frac{1}{2},j+\frac{1}{2}}}$, ▲ for $E^f_{y_{i,j+\frac{1}{2}}}$ and $J^f_{y_{i,j+\frac{1}{2}}}$, ▼ for $E^f_{x_{i+\frac{1}{2},j}}$ and $J^f_{x_{i+\frac{1}{2},j}}$.

*2.2. Some notations*

Divide domain $\Omega$ into two sub-domains, i.e. $\bar{\Omega} = \bar{\Omega}^c \cup \bar{\Omega}^f$, with the interface $\Gamma = \bar{\Omega}^c \cap \bar{\Omega}^f$, where $\Omega^c$ denotes the coarse grid sub-domain and $\Omega^f$ represents the fine grid sub-domain. We take the $1:2$ local mesh refinement of staggered mesh to domain $\Omega$ as shown in Fig. 1. Let $\Delta x$ and $\Delta y$ be the fine mesh sizes along $x$- and $y$- directions for the fine sub-domain, let $2\Delta x$ and $2\Delta y$ be the coarse mesh sizes along $x$- and $y$- directions for the coarse sub-domain.

Let mesh points on $\Omega^c$ be

$$x^c_i = a + i(2\Delta x),\ 0 \le i \le I^{int};\ y^c_j = c + j(2\Delta y), 0 \le j \le J_c;$$

$$x^c_{i+\frac{1}{2}} = a + (i+\frac{1}{2})(2\Delta x),\ 0 \le i \le I^{int} - 1;\ y^c_{j+\frac{1}{2}} = c + (j+\frac{1}{2})(2\Delta y),\ 0 \le j \le J_c - 1;$$

and let mesh points on $\Omega^f$ be

$$x^f_i = x^c_{I^{int}} + (i - I^{int})(\Delta x), I^{int} \le i \le I;\ y^f_j = c + j(\Delta y), 0 \le j \le J_f;$$

$$x_i^f = x_{I^{int}}^c + (i - I^{int} + \frac{1}{2})(\Delta x), I^{int} \le i \le I-1;\ y_{j+\frac{1}{2}}^f = c + (j+\frac{1}{2})(\Delta y), 0 \le j \le J_f - 1.$$

Define the layered domain refinement as

$$\Omega_{h,E_x^c} = \{(x_{i+\frac{1}{2}}, y_j)|_{i=0,j=0}^{I^{int}-1,J_c}\}, \Omega_{h,E_y^c} = \{(x_i, y_{j+\frac{1}{2}})|_{i=0,j=0}^{I^{int},J_c-1}\}, \Omega_{h,H_z^c} = \{(x_{i+\frac{1}{2}}, y_{j+\frac{1}{2}})|_{i=0,j=0}^{I^{int},J_c-1}\},$$
$$\Omega_{h,E_x^f} = \{(x_{i+\frac{1}{2}}, y_j)|_{i=I^{int},j=0}^{I-1,J_f}\}, \Omega_{h,E_y^f} = \{(x_i, y_{j+\frac{1}{2}})|_{i=I^{int},j=0}^{I,J_f-1}\}, \Omega_{h,H_z^f} = \{(x_{i+\frac{1}{2}}, y_{j+\frac{1}{2}})|_{i=I^{int},j=0}^{I,J_f-1}\},$$
$$\Omega_{h,J_x^c} = \{(x_{i+\frac{1}{2}}, y_j)|_{i=0,j=0}^{I^{int}-1,J_c}\}, \Omega_{h,J_y^c} = \{(x_i, y_{j+\frac{1}{2}})|_{i=0,j=0}^{I^{int},J_c-1}\}, \Omega_{h,K_z^c} = \{(x_{i+\frac{1}{2}}, y_{j+\frac{1}{2}})|_{i=0,j=0}^{I^{int},J_c-1}\},$$
$$\Omega_{h,J_x^f} = \{(x_{i+\frac{1}{2}}, y_j)|_{i=I^{int},j=0}^{I-1,J_f}\}, \Omega_{h,J_y^f} = \{(x_i, y_{j+\frac{1}{2}})|_{i=I^{int},j=0}^{I,J_f-1}\}, \Omega_{h,K_z^f} = \{(x_{i+\frac{1}{2}}, y_{j+\frac{1}{2}})|_{i=I^{int},j=0}^{I,J_f-1}\}.$$

Define time step size as $\Delta t = \frac{T}{N}$ and $t^n = n\Delta t$, $0 \le n \le N$. Let grid functions $\{E_{x_{i+\frac{1}{2},j}}^c, E_{y_{i,j+\frac{1}{2}}}^c, H_{z_{i+\frac{1}{2},j+\frac{1}{2}}}^c, J_{x_{i+\frac{1}{2},j}}^c, J_{y_{i,j+\frac{1}{2}}}^c, K_{z_{i+\frac{1}{2},j+\frac{1}{2}}}^c\}$ on $\Omega_h^c$ and $\{E_{x_{i+\frac{1}{2},j}}^f, E_{y_{i,j+\frac{1}{2}}}^f, H_{z_{i+\frac{1}{2},j+\frac{1}{2}}}^f, J_{x_{i+\frac{1}{2},j}}^f, J_{y_{i,j+\frac{1}{2}}}^f, K_{z_{i+\frac{1}{2},j+\frac{1}{2}}}^f\}$ on $\Omega_h^f$. The difference operators are defined as

$$\delta_x^c U_{\alpha,\beta}^{c,n} = \frac{1}{2\Delta x}(U_{\alpha+1/2,\beta}^{c,n} - U_{\alpha-1/2,\beta}^{c,n}),\ \delta_y^c U_{\alpha,\beta}^{c,n} = \frac{1}{2\Delta y}(U_{\alpha,\beta+1/2}^{c,n} - U_{\alpha,\beta-1/2}^{c,n}),$$
$$\delta_x^f U_{\alpha,\beta}^{f,n} = \frac{1}{\Delta x}(U_{\alpha+1/2,\beta}^{f,n} - U_{\alpha-1/2,\beta}^{f,n}),\ \delta_y^f U_{\alpha,\beta}^{f,n} = \frac{1}{\Delta y}(U_{\alpha,\beta+1/2}^{f,n} - U_{\alpha,\beta-1/2}^{f,n}),$$
$$\delta_t U_{\alpha,\beta}^{c,n} = \frac{1}{\Delta t}(U_{\alpha,\beta}^{c,n+1/2} - U_{\alpha,\beta}^{c,n-1/2}),\ \delta_t U_{\alpha,\beta}^{f,n} = \frac{1}{\Delta t}(U_{\alpha,\beta}^{f,n+1/2} - U_{\alpha,\beta}^{f,n-1/2}),$$

where $\alpha = i$ or $i+\frac{1}{2}$, $\beta = j$ or $j+\frac{1}{2}$, and $r = c$ or $f$ represents domain restricted to coarse or refined region respectively.

## 3. The GEP-LMR-S-FDTD-I scheme and fast implementation

For constructing the energy-conserved scheme on both coarse and fine meshes, we split the system (16) - (24) into a two stage process of sub-systems along $x-$ and $y-$ directions in each time interval $(t^n, t^{n+1}]$

$$\begin{cases} \epsilon_0 \dfrac{\partial E_y}{\partial t} = -\dfrac{\partial H_z}{\partial x} - J_y, \\ \mu_0 \dfrac{\partial H_z}{\partial t} = -\dfrac{\partial E_y}{\partial x} - K_z, \\ \gamma_e \dfrac{\partial J_y}{\partial t} + \gamma_e \Gamma_e J_y = E_y, \\ \gamma_m \dfrac{\partial K_z}{\partial t} + \gamma_m \Gamma_m K_z = H_z, \end{cases} \qquad \begin{cases} \epsilon_0 \dfrac{\partial E_x}{\partial t} = \dfrac{\partial H_z}{\partial y} - J_x, \\ \mu_0 \dfrac{\partial H_z}{\partial t} = \dfrac{\partial E_x}{\partial y}, \\ \gamma_e \dfrac{\partial J_x}{\partial t} + \gamma_e \Gamma_e J_x = E_x. \end{cases} \tag{26}$$

### *3.1. The GEP-LMR-S-FDTD-I scheme*

Over domain refinement in Fig. 1, we first solve $E_y^{n+1}$,$H_z^*$,$J_y^{n+1}$,$K_z^{n+1}$, in $x$-direction at Stage 1 and then calculate $E_x^{n+1}$,$H_z^{n+1}$,$J_x^{n+1}$ along $y$-direction at Stage 2. The significance of the scheme proposed below is that the local interface equations ensure global energy conservation. The global energy-preserving local mesh refined splitting FTDT scheme (GEP-LMR-S-FDTD-I) is proposed as: For $n = 0, 1, \cdots, N-1$ do

**Stage 1**: Solve $E_y^{c,n+1}$,$H_z^{c,*}$, $E_y^{f,n+1}$,$H_z^{f,*}$,$J_y^{c,n+1}$,$K_z^{c,n+1}$,$J_y^{f,n+1}$,$K_z^{f,n+1}$ along $x$-direction for $j = 0, 1, \cdots, J_c - 1$

(1-a). On coarse sub-domain $\Omega_h^c$, compute $E_y^{c,n+1}$, intermediate variable $H_z^{c,*}$, $J_y^{c,n+1}$ and $K_z^{c,n+1}$ by

$$\epsilon_0\frac{E^{c,n+1}_{y_{i,j+1/2}}-E^{c,n}_{y_{i,j+1/2}}}{\Delta t}=-\frac{1}{2}\delta_x^c\{H^{c,*}_{z_{i,j+1/2}}+H^{c,n}_{z_{i,j+1/2}}\}-\frac{1}{2}\{J^{c,n}_{y_{i,j+1/2}}+J^{c,n+1}_{y_{i,j+1/2}}\},\tag{27}$$

$$\mu_0\frac{H^{c,*}_{z_{i+1/2,j+1/2}}-H^{c,n}_{z_{i+1/2,j+1/2}}}{\Delta t}=-\frac{1}{2}\delta_x^c\{E^{c,n+1}_{y_{i+1/2,j+1/2}}+E^{c,n}_{y_{i+1/2,j+1/2}}\}-\frac{1}{2}\{K^{c,n}_{z_{i+1/2,j+1/2}}+K^{c,n+1}_{z_{i+1/2,j+1/2}}\},\tag{28}$$

$$\gamma_e\frac{J^{c,n+1}_{y_{i,j+1/2}}-J^{c,n}_{y_{i,j+1/2}}}{\Delta t}+\gamma_e\Gamma_e\frac{1}{2}\{J^{c,n+1}_{y_{i,j+1/2}}+J^{c,n}_{y_{i,j+1/2}}\}=\frac{1}{2}\{E^{c,n+1}_{y_{i,j+1/2}}+E^{c,n}_{y_{i,j+1/2}}\},\tag{29}$$

$$\gamma_m\frac{K^{c,n+1}_{z_{i+1/2,j+1/2}}-K^{c,n}_{z_{i+1/2,j+1/2}}}{\Delta t}+\gamma_m\Gamma_m\frac{1}{2}\{K^{c,n+1}_{z_{i+1/2,j+1/2}}+K^{c,n}_{z_{i+1/2,j+1/2}}\}=\frac{1}{2}\{H^{c,n+1}_{z_{i+1/2,j+1/2}}+H^{c,n}_{z_{i+1/2,j+1/2}}\},\tag{30}$$

$$for\ i=0,1,\cdots,I^{int}-1$$

(1-b). On refined sub-domain $\Omega_h^f$, compute $E_y^{f,n+1}$, intermediate variable $H_z^{f,*}$, $J_y^{f,n+1}$ and $K_z^{f,n+1}$ by

$$\epsilon_0\frac{E^{f,n+1}_{y_{i,j+1/2}}-E^{f,n}_{y_{i,j+1/2}}}{\Delta t}=-\frac{1}{2}\delta_x^f\{H^{f,*}_{z_{i,j+1/2}}+H^{f,n}_{z_{i,j+1/2}}\}-\frac{1}{2}\{J^{f,n}_{y_{i,j+1/2}}+J^{f,n+1}_{y_{i,j+1/2}}\},\tag{31}$$

$$\mu_0\frac{H^{f,*}_{z_{i+1/2,j+1/2}}-H^{f,n}_{z_{i+1/2,j+1/2}}}{\Delta t}=-\frac{1}{2}\delta_x^f\{E^{f,n+1}_{y_{i+1/2,j+1/2}}+E^{f,n}_{y_{i+1/2,j+1/2}}\}-\frac{1}{2}\{K^{f,n}_{z_{i+1/2,j+1/2}}+K^{f,n+1}_{z_{i+1/2,j+1/2}}\},\tag{32}$$

$$\gamma_e\frac{J^{f,n+1}_{y_{i,j+1/2}}-J^{f,n}_{y_{i,j+1/2}}}{\Delta t}+\gamma_e\Gamma_e\frac{1}{2}\{J^{f,n+1}_{y_{i,j+1/2}}+J^{f,n}_{y_{i,j+1/2}}\}=\frac{1}{2}\{E^{f,n+1}_{y_{i,j+1/2}}+E^{f,n}_{y_{i,j+1/2}}\},\tag{33}$$

$$\gamma_m\frac{K^{f,n+1}_{z_{i+1/2,j+1/2}}-K^{f,n}_{z_{i+1/2,j+1/2}}}{\Delta t}+\gamma_m\Gamma_m\frac{1}{2}\{K^{f,n+1}_{z_{i+1/2,j+1/2}}+K^{f,n}_{z_{i+1/2,j+1/2}}\}=\frac{1}{2}\{H^{f,n+1}_{z_{i+1/2,j+1/2}}+H^{f,n}_{z_{i+1/2,j+1/2}}\},\tag{34}$$

$$for\ \ i=I^{int}+1,I^{int}+2,\cdots,I-1$$

(1-c). On interface $\Gamma$ of $\Omega_h^c$ and $\Omega_h^f$, at $i=I^{int}$

$$\begin{aligned}&-2\epsilon_0\Delta x\delta_t E^{c,n+1/2}_{y_{I^{int},j+1/2}}+\{H^{c,*}_{z_{I^{int}-1/2,j+1/2}}+H^{c,n}_{z_{I^{int}-1/2,j+1/2}}\}-\Delta x(J^{c,n+1}_{y_{I^{int},j+1/2}}+J^{c,n}_{y_{I^{int},j+1/2}})\\&\quad=\epsilon_0\Delta x\delta_t E^{f,n+1/2}_{y_{I^{int},2j+1/2}}+\{H^{f,*}_{z_{I^{int}+1/2,2j+1/2}}+H^{f,n}_{z_{I^{int}+1/2,2j+1/2}}\}+\frac{1}{2}\Delta x(J^{f,n+1}_{y_{I^{int},2j+1/2}}+J^{f,n}_{y_{I^{int},2j+1/2}}),\end{aligned}\tag{35}$$

$$E^{c,n+1}_{y_{I^{int},j+1/2}}+E^{c,n}_{y_{I^{int},j+1/2}}=\frac{1}{2}\{E^{f,n+1}_{y_{I^{int},2j+1/2}}+E^{f,n}_{y_{I^{int},2j+1/2}}\}+\frac{1}{2}\{E^{f,n+1}_{y_{I^{int},2j+3/2}}+E^{f,n}_{y_{I^{int},2j+3/2}}\}\tag{36}$$

$$\begin{aligned}&-2\epsilon_0\Delta x\delta_t E^{c,n+1/2}_{y_{I^{int},j+1/2}}+\{H^{c,*}_{z_{I^{int}-1/2,j+1/2}}+H^{c,n}_{z_{I^{int}-1/2,j+1/2}}\}-\Delta x(J^{c,n+1}_{y_{I^{int},j+1/2}}+J^{c,n}_{y_{I^{int},j+1/2}})\\&\quad=\epsilon_0\Delta x\delta_t E^{f,n+1/2}_{y_{I^{int},2j+3/2}}+\{H^{f,*}_{z_{I^{int}+1/2,2j+3/2}}+H^{f,n}_{z_{I^{int}+1/2,2j+3/2}}\}+\frac{1}{2}\Delta x(J^{f,n+1}_{y_{I^{int},2j+3/2}}+J^{f,n}_{y_{I^{int},2j+3/2}}).\end{aligned}\tag{37}$$

**Stage2**: Solve $E_x^{c,n+1}$, $H_z^{c,n+1}$, $J_x^{c,n+1}$ and $E_x^{f,n+1}$, $H_z^{f,n+1}$, $J_x^{f,n+1}$ along $y$-direction.

(2-a). On coarse sub-domain $\Omega_h^c$, compute $E_x^{c,n+1}$, $H_z^{c,n+1}$, $J_x^{c,n+1}$ for $i=0,1,\cdots,I^{int}-1$

$$\epsilon_0\frac{E^{c,n+1}_{x_{i+1/2,j}}-E^{c,n}_{x_{i+1/2,j}}}{\Delta t}=\frac{1}{2}\delta_y^c\{H^{c,*}_{z_{i+1/2,j}}+H^{c,n}_{z_{i+1/2,j}}\}-\frac{1}{2}\{J^{c,n}_{x_{i+1/2,j}}+J^{c,n+1}_{x_{i+1/2,j}}\},\tag{38}$$

$$\mu_0\frac{H^{c,n+1}_{z_{i+1/2,j+1/2}}-H^{c,*}_{z_{i+1/2,j+1/2}}}{\Delta t}=\frac{1}{2}\delta_y^c\{E^{c,n+1}_{x_{i+1/2,j+1/2}}+E^{c,n}_{x_{i+1/2,j+1/2}}\},\tag{39}$$

$$\gamma_e\frac{J^{c,n+1}_{x_{i+1/2,j}}-J^{c,n}_{x_{i+1/2,j}}}{\Delta t}+\gamma_e\Gamma_e\frac{1}{2}\{J^{c,n+1}_{x_{i+1/2,j}}+J^{c,n}_{x_{i+1/2,j}}\}=\frac{1}{2}\{E^{c,n+1}_{x_{i+1/2,j}}+E^{c,n}_{x_{i+1/2,j}}\},\tag{40}$$

$$for\ \ j=0,1,\cdots,J_c-1$$

(2-b). On refined sub-domain $\Omega_h^f$, compute $E_x^{f,n+1}$, $H_z^{f,n+1}$, $J_x^{f,n+1}$ for $i = I^{int}, I^{int}+1, \cdots, I-1$

$$\epsilon_0 \frac{E^{f,n+1}_{x_{i+1/2,j}} - E^{f,n}_{x_{i+1/2,j}}}{\Delta t} = \frac{1}{2}\delta_y^f \{H^{f,*}_{z_{i+1/2,j}} + H^{f,n}_{z_{i+1/2,j}}\} - \frac{1}{2}\{J^{f,n}_{x_{i+1/2,j}} + J^{f,n+1}_{x_{i+1/2,j}}\}, \tag{41}$$

$$\mu_0 \frac{H^{f,n+1}_{z_{i+1/2,j+1/2}} - H^{f,*}_{z_{i+1/2,j+1/2}}}{\Delta t} = \frac{1}{2}\delta_y^f \{E^{f,n+1}_{y_{i+1/2,j+1/2}} + E^{f,n}_{y_{i+1/2,j+1/2}}\}, \tag{42}$$

$$\gamma_e \frac{J^{f,n+1}_{x_{i+1/2,j}} - J^{f,n}_{x_{i+1/2,j}}}{\Delta t} + \gamma_e \Gamma_e \frac{1}{2}\{J^{f,n+1}_{x_{i+1/2,j}} + J^{f,n}_{x_{i+1/2,j}}\} = \frac{1}{2}\{E^{f,n+1}_{x_{i+1/2,j}} + E^{f,n}_{x_{i+1/2,j}}\}, \tag{43}$$

$$for \quad j = 0, 1, \cdots, J_f - 1.$$

And PEC boundary condition and initial values are provided.

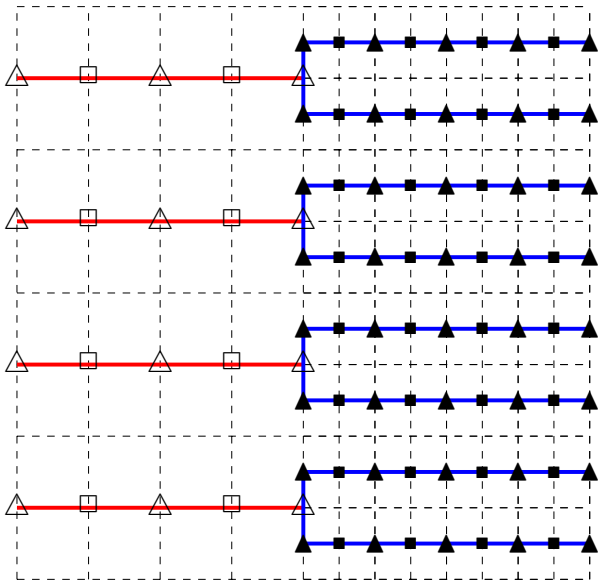

Figure 2: Diagram of computation for the GEC-LMR-S-FDTD-I scheme at Stage 1 along $x$-direction.

*3.2. Fast implementation*

At Stage 1 of the GEP-LMR-S-FDTD-I scheme, for $j = 0, 1, \cdots, J_c - 1$, first we substitute $K_z^{c,n+1}$ of (30) into (28) to form equations of $H_z^{c,*}$, and we then substitute $H_z^{c,*}$ and $J_y^{c,n+1}$ of (29) into (27) to form equations of $E_y^{c,n+1}$. Similarly, for the refined sub-domain equations (31)-(34), we form equations of $E_y^{f,n+1}$. And together with interface equations (35)-(37), the Stage 1 leads to solve unknown variables $\{E^{c,n+1}_{y_{i,j+\frac{1}{2}}}, E^{f,n+1}_{y_{i,2j+\frac{1}{2}}}, E^{f,n+1}_{y_{i,2j+\frac{3}{2}}}\}$ in a "trifuecate" structure for each $j$ (see Fig. 2). The corresponding matrix system for each $j$ is complicated, it cannot be efficiently solved. We propose a fast implementation of the systems to overcome this issue by transferring the "trifuecate" structure into a "line" structure and an "inverted U" structure. To begin with, consider the interface calculation. First, substituting $K^{c,n+1}_{z_{I^{int}-\frac{1}{2},j+\frac{1}{2}}}$ from equation (30) into $H^{c,*}_{z_{I^{int}-\frac{1}{2},j+\frac{1}{2}}}$ in equation (28) at point i = $I^{int}$ - 1 and $H^{f,*}_{z_{I^{int}+\frac{1}{2},2j+\frac{1}{2}}}$, $H^{f,*}_{z_{I^{int}+\frac{1}{2},2j+\frac{3}{2}}}$ from equations (32) and (34) at point i = $I^{int}$. Then substituting those values in interface equations (35) and (37), and substitute $J^{c,n+1}_{y_{I^{int},j+\frac{1}{2}}}$ and $J^{f,n+1}_{y_{I^{int},2j+\frac{1}{2}}}$,$J^{f,n+1}_{y_{I^{int},2j+\frac{3}{2}}}$ from

equations (29) and (33) into interface equations (35) and (37) we can obtain that

$$\begin{aligned}
&(-2\epsilon_0\frac{\Delta x}{\Delta t}-\frac{c}{4\Delta x}-\frac{\Delta xe}{2})E^{c,n+1}_{y_{Iint,j+\frac{1}{2}}}-(\epsilon_0\frac{\Delta x}{\Delta t}+\frac{c}{2\Delta x}-\frac{\Delta xe}{4})E^{f,n}_{y_{Iint,2j+\frac{1}{2}}}+\frac{c}{2\Delta x}E^{f,n+1}_{y_{Iint+1,2j+\frac{1}{2}}}\\
&=(-2\epsilon_0\frac{\Delta x}{\Delta t}+\frac{c}{4\Delta x}+\frac{\Delta xe}{2})E^{c,n}_{y_{Iint,j+\frac{1}{2}}}+(-\epsilon_0\frac{\Delta x}{\Delta t}+\frac{c}{2\Delta x}+\frac{\Delta xe}{4})E^{f,n}_{y_{Iint,2j+\frac{1}{2}}}-\frac{c}{2\Delta x}E^{f,n}_{y_{Iint+1,2j+\frac{1}{2}}}\\
&-\frac{c}{4\Delta x}E^{c,n+1}_{y_{Iint-1,j+\frac{1}{2}}}-\frac{c}{2}(ab+1)(K^{f,n}_{z_{Iint+\frac{1}{2},2j+\frac{1}{2}}}-K^{c,n}_{z_{Iint-\frac{1}{2},j+\frac{1}{2}}})\\
&+\frac{\Delta x}{2}(ef+1)(J^{f,n}_{y_{Iint,2j+\frac{1}{2}}}+2J^{c,n}_{y_{Iint,j+\frac{1}{2}}})+(cd+1)(H^{f,n}_{z_{Iint+\frac{1}{2},2j+\frac{1}{2}}}-H^{c,n}_{z_{Iint-\frac{1}{2},j+\frac{1}{2}}})
\end{aligned}\tag{44}$$

$$E^{c,n+1}_{y_{Iint,j+1/2}}+E^{c,n}_{y_{Iint,j+1/2}}=\frac{1}{2}\{E^{f,n+1}_{y_{Iint,2j+1/2}}+E^{f,n}_{y_{Iint,2j+1/2}}\}+\frac{1}{2}\{E^{f,n+1}_{y_{Iint,2j+3/2}}+E^{f,n}_{y_{Iint,2j+3/2}}\}\tag{45}$$

$$\begin{aligned}
&(-2\epsilon_0\frac{\Delta x}{\Delta t}-\frac{c}{4\Delta x}-\frac{\Delta xe}{2})E^{c,n+1}_{y_{Iint,j+\frac{1}{2}}}-(\epsilon_0\frac{\Delta x}{\Delta t}+\frac{c}{2\Delta x}-\frac{\Delta xe}{4})E^{f,n}_{y_{Iint,2j+\frac{3}{2}}}+\frac{c}{2\Delta x}E^{f,n+1}_{y_{Iint+1,2j+\frac{3}{2}}}\\
&=(-2\epsilon_0\frac{\Delta x}{\Delta t}+\frac{c}{4\Delta x}+\frac{\Delta xe}{2})E^{c,n}_{y_{Iint,j+\frac{1}{2}}}+(-\epsilon_0\frac{\Delta x}{\Delta t}+\frac{c}{2\Delta x}+\frac{\Delta xe}{4})E^{f,n}_{y_{Iint,2j+\frac{3}{2}}}-\frac{c}{2\Delta x}E^{f,n}_{y_{Iint+1,2j+\frac{3}{2}}}\\
&-\frac{c}{4\Delta x}E^{c,n+1}_{y_{Iint-1,j+\frac{1}{2}}}-\frac{c}{2}(ab+1)(K^{f,n}_{z_{Iint+\frac{1}{2},2j+\frac{3}{2}}}-K^{c,n}_{z_{Iint-\frac{1}{2},j+\frac{1}{2}}})\\
&+\frac{\Delta x}{2}(ef+1)(J^{f,n}_{y_{Iint,2j+\frac{3}{2}}}+2J^{c,n}_{y_{Iint,j+\frac{1}{2}}})+(cd+1)(H^{f,n}_{z_{Iint+\frac{1}{2},2j+\frac{3}{2}}}-H^{c,n}_{z_{Iint-\frac{1}{2},j+\frac{1}{2}}})
\end{aligned}\tag{46}$$

We define the average of variables on fined sub-domain as

$$\overline{E}^{f,n+1}_{y_{i,2j+1}}=(E^{f,n+1}_{y_{i,2j+\frac{1}{2}}}+E^{f,n+1}_{y_{i,2j+\frac{3}{2}}})/2,\qquad \overline{H}^{f,n+1}_{z_{i+\frac{1}{2},2j+1}}=(H^{f,n+1}_{z_{i+\frac{1}{2},2j+\frac{1}{2}}}+H^{f,n+1}_{z_{i+\frac{1}{2},2j+\frac{3}{2}}})/2\tag{47}$$

$$\overline{J}^{f,n+1}_{y_{i,2j+1}}=(J^{f,n+1}_{y_{i,2j+\frac{1}{2}}}+J^{f,n+1}_{y_{i,2j+\frac{3}{2}}})/2,\qquad \overline{K}^{f,n+1}_{z_{i+\frac{1}{2},2j+1}}=(K^{f,n+1}_{z_{i+\frac{1}{2},2j+\frac{1}{2}}}+K^{f,n+1}_{z_{i+\frac{1}{2},2j+\frac{3}{2}}})/2.\tag{48}$$

Adding interface equations (35) and (37), it gets that

$$\begin{aligned}
&-4\epsilon_0\Delta x\delta_t E^{c,n+1/2}_{y_{Iint,j+1/2}}+2\{H^{c,*}_{z_{Iint-1/2,j+1/2}}+H^{c,n}_{z_{Iint-1/2,j+1/2}}\}-2\Delta x(J^{c,n+1}_{y_{Iint,j+1/2}}+J^{c,n}_{y_{Iint,j+1/2}})\\
&=2\epsilon_0\Delta x\delta_t\overline{E}^{f,n+1/2}_{y_{Iint,2j+1/2}}+2\{\overline{H}^{f,*}_{z_{Iint+1/2,2j+1/2}}+\overline{H}^{f,n}_{z_{Iint+1/2,2j+1/2}}\}+\Delta x(\overline{J}^{f,n+1}_{y_{Iint,2j+1/2}}+\overline{J}^{f,n}_{y_{Iint,2j+1/2}}).
\end{aligned}\tag{49}$$

Adding interface equations (44) and (46), it gets that

$$\begin{aligned}
&(-4\epsilon_0\frac{\Delta x}{\Delta t}-\frac{c}{2\Delta x}-\Delta xe)E^{c,n+1}_{y_{Iint,j+\frac{1}{2}}}-(2\epsilon_0\frac{\Delta x}{\Delta t}+\frac{c}{\Delta x}-\frac{\Delta xe}{2})\overline{E}^{f,n+1}_{y_{Iint,2j+1}}+\frac{c}{\Delta x}\overline{E}^{f,n+1}_{y_{Iint+1,2j+1}}\\
&=(-4\epsilon_0\frac{\Delta x}{\Delta t}+\frac{c}{2\Delta x}+\Delta xe)E^{c,n}_{y_{Iint,j+\frac{1}{2}}}+(-2\epsilon_0\frac{\Delta x}{\Delta t}+\frac{c}{\Delta x}+\frac{\Delta xe}{2})\overline{E}^{f,n}_{y_{Iint,2j+1}}\\
&-\frac{c}{\Delta x}\overline{E}^{f,n}_{y_{Iint+1,2j+1}}-\frac{c}{2\Delta x}E^{c,n+1}_{y_{Iint-1,j+\frac{1}{2}}}-\frac{c}{2\Delta x}E^{c,n}_{y_{Iint-1,j+\frac{1}{2}}}-c(ab+1)(\overline{K}^{f,n}_{z_{Iint+\frac{1}{2},2j+1}}-K^{c,n}_{z_{Iint-\frac{1}{2},j+\frac{1}{2}}})\\
&+\Delta x(ef+1)(\overline{J}^{f,n}_{y_{Iint+\frac{1}{2},2j+1}}+2J^{c,n}_{y_{Iint+\frac{1}{2},j+\frac{1}{2}}})+2(cd+1)(\overline{H}^{f,n}_{z_{Iint+\frac{1}{2},2j+1}}-H^{c,n}_{z_{Iint-\frac{1}{2},j+\frac{1}{2}}})
\end{aligned}\tag{50}$$

Substituting $H^*_z$ and $J^{n+1}_y$ of (29) and (33), similarly treating to equations (31)-(34), and using (36) by

$$E^{c,n+1}_{Iint,j+\frac{1}{2}}=\overline{E}^{f,n+1}_{y_{Iint,2j+1}}+\overline{E}^{f,n}_{y_{Iint,2j+1}}-E^{c,n}_{Iint,j+\frac{1}{2}},\tag{51}$$

we finally

$$
\begin{aligned}
&(-6\epsilon_0\frac{\Delta x}{\Delta t}-\frac{3c}{2\Delta x}-\frac{3\Delta xe}{2})\overline{E}^{f,n+1}_{y_{Iint,2j+1}}+\frac{c}{\Delta x}\overline{E}^{f,n+1}_{y_{Iint+1,2j+1}}+\frac{c}{2\Delta x}E^{c,n+1}_{y_{Iint-1,j+\frac{1}{2}}}\\
&=(2\epsilon_0\frac{\Delta x}{\Delta t}+\frac{3c}{2\Delta x}+\frac{3\Delta xe}{2})\overline{E}^{f,n}_{y_{Iint,2j+1}}-8\epsilon_0\frac{\Delta x}{\Delta t}E^{c,n}_{y_{Iint,j+\frac{1}{2}}}-\frac{c}{\Delta x}\overline{E}^{f,n}_{y_{Iint+1,2j+1}}-\frac{c}{2\Delta x}E^{c,n}_{y_{Iint-1,j+\frac{1}{2}}}\\
&\quad-c(ab+1)(\overline{K}^{f,n}_{z_{Iint+\frac{1}{2},2j+1}}-K^{c,n}_{z_{Iint-\frac{1}{2},j+\frac{1}{2}}})\\
&\quad+\Delta x(ef+1)(\overline{J}^{f,n}_{y_{Iint+\frac{1}{2},2j+1}}+2J^{c,n}_{y_{Iint+\frac{1}{2},j+\frac{1}{2}}})+2(cd+1)(\overline{H}^{f,n}_{z_{Iint+\frac{1}{2},2j+1}}-H^{c,n}_{z_{Iint-\frac{1}{2},j+\frac{1}{2}}})
\end{aligned}
\tag{52}
$$

Where,

$$
a=\frac{1}{\frac{\gamma_m}{\Delta t}+\frac{\gamma_m\Gamma_m}{2}},b=\frac{\gamma_m}{\Delta t}-\frac{\gamma_m\Gamma_m}{2},c=\frac{1}{\frac{\mu}{\Delta t}+\frac{a}{4}},d=\frac{\mu}{\Delta t}-\frac{a}{4},e=\frac{1}{\frac{\gamma_e}{\Delta t}+\frac{\gamma_e\Gamma_e}{2}},f=\frac{\gamma_e}{\Delta t}-\frac{\gamma_e\Gamma_e}{2}
$$

by treating unknowns of coarse grid points from equations (27)-(30) as well as unknowns of fine grid points from equations (31)-(34) together with knowns of equation (52) get a tridiagonal system of unknowns of $(E^{c,n+1}_{y_{1,j+\frac{1}{2}}}, E^{c,n+1}_{y_{2,j+\frac{1}{2}}}, \cdots, E^{c,n+1}_{y_{Iint-1,j+\frac{1}{2}}}, \overline{E}^{f,n+1}_{y_{Iint,2j+1}}, \overline{E}^{f,n+1}_{y_{Iint+1,2j+1}}, \cdots, \overline{E}^{f,n+1}_{y_{I-1,2j+1}})^\tau$ in a line structure for each $j$ (see redlines of Fig. 2), which can be efficiently solved by Thomas' algorithm. Then we solve interface value $E^{c,n+1}_{y_{Iint,j+\frac{1}{2}}}$ and refined sub-domain unknowns $E^{f,n+1}_{y_{i,2j+\frac{1}{2}}}$ and $E^{f,n+1}_{y_{i,2j+\frac{3}{2}}}$ in an "inverted U" structure for each $j$, which leads to another tridiagonal system of unknowns (see bluelines of Fig. 2) and it can be computed by Thomas' algorithm. The unknowns of $H^{c,*}_z$, $K^{c,n+1}_z$, $J^{c,n+1}_y$ and $H^{f,*}_z$, $J^{f,n+1}_y$ and $K^{f,n+1}_z$ are then directly solve for Stage 1. Since there is no interface involved in $y$-direction, Stage 2 leads tridiagonal systems and can be easily solved.

**Algorithm 1** Fast Implementation of GEP-LMR-S-FDTD-I

```
Initialize;
for n = 1,...,N do
    for j = 1,...,J_c − 1 do
        Solve E_y^{c,n+1} and Ē_y^{f,n+1} along straight "line" structure for each i
        Solve E_{y_{i,2j+1/2}}^{f,n+1}, E_{y_{i,2j+3/2}}^{f,n+1} and E_{y_{Iint,j}}^{c,n+1} along "inverted U" structure for
    each i
        Update H_z^{c,*}, H_z^{f,*}, K_z^{c,n+1}, K_z^{f,n+1}, J_y^{c,n+1} and J_y^{f,n+1} by E_y^{c,n+1} and E_y^{f,n+1}
    end for
    for i = 1,...,I − 1 do
        Solve E_x^{c,n+1} and E_x^{f,n+1} along y direction for each j
        Update H_z^{c,n+1}, H_z^{f,n+1}, , J_x^{c,n+1}, J_x^{f,n+1} by E_x^{c,n+1} and E_x^{f,n+1}
    end for
end for
```

## 4. The GEP-LMR-S-FDTD-II scheme

The GEP-LMR-S-FDTD-I is based on the first order time splitting process and thus is of first order accuracy in time. In this section, we further propose the global energy preserving local mesh refined scheme by applying for the second order time splitting process of operator to Maxwell's equations in Drude metamaterials.

The GEP-LMR-S-FDTD-II scheme is proposed as: For $n = 0, 1, \cdots, N-1$ do

**Stage 1**: Along $y$-direction, solve $E_x^{c,*}$, $J_x^{c,*}$, $H_z^{c,*}$ and $E_x^{f,*}$, $J_x^{f,*}$, $H_z^{f,*}$.

(1-a). On coarse sub-domain $\Omega_h^c$, compute $E_x^{c,*}$, $J_x^{c,*}$ and $H_z^{c,*}$ from $E_x^{c,n}$, $J_x^{c,n}$ and $H_z^{c,n}$ for $i = 0, 1, \cdots, I^{int}-1$

$$\epsilon_0 \frac{E^{c,*}_{x_{i+1/2,j}} - E^{c,n}_{x_{i+1/2,j}}}{\Delta t} = \frac{1}{4}\delta_y^c \{H^{c,*}_{z_{i+1/2,j}} + H^{c,n}_{z_{i+1/2,j}}\} - \frac{1}{4}\{J^{c,n}_{x_{i+1/2,j}} + J^{c,*}_{x_{i+1/2,j}}\} \tag{53}$$

$$\mu_0 \frac{H^{c,*}_{z_{i+1/2,j+1/2}} - H^{c,n}_{z_{i+1/2,j+1/2}}}{\Delta t} = \frac{1}{4}\delta_y^c \{E^{c,*}_{x_{i+1/2,j+1/2}} + E^{c,n}_{x_{i+1/2,j+1/2}}\} \tag{54}$$

$$\gamma_e \frac{J^{c,*}_{x_{i+1/2,j}} - J^{c,n}_{x_{i+1/2,j}}}{\Delta t} + \frac{\gamma_e \Gamma_e}{4}\{J^{c,*}_{x_{i+1/2,j}} + J^{c,n}_{x_{i+1/2,j}}\} = \frac{1}{4}\{E^{c,*}_{x_{i+1/2,j}} + E^{c,n}_{x_{i+1/2,j}}\} \tag{55}$$

(1-b). On refined sub-domain $\Omega_h^f$, compute $E_x^{f,*}$, $J_x^{f,*}$, $H_z^{f,*}$ from $E_x^{f,n}$, $J_x^{f,n}$ and $H_z^{f,n}$ for $i = I^{int}, I^{int}+1, \cdots, I-1$

$$\epsilon_0 \frac{E^{f,*}_{x_{i+1/2,j}} - E^{f,n}_{x_{i+1/2,j}}}{\Delta t} = \frac{1}{4}\delta_y^f \{H^{f,*}_{z_{i+1/2,j}} + H^{f,n}_{z_{i+1/2,j}}\} - \frac{1}{4}\{J^{f,n}_{x_{i+1/2,j}} + J^{f,*}_{x_{i+1/2,j}}\} \tag{56}$$

$$\mu_0 \frac{H^{f,*}_{z_{i+1/2,j+1/2}} - H^{f,n}_{z_{i+1/2,j+1/2}}}{\Delta t} = \frac{1}{4}\delta_y^f \{E^{f,*}_{x_{i+1/2,j+1/2}} + E^{f,n}_{x_{i+1/2,j+1/2}}\} \tag{57}$$

$$\gamma_e \frac{J^{f,*}_{x_{i+1/2,j}} - J^{f,n}_{x_{i+1/2,j}}}{\Delta t} + \frac{\gamma_e \Gamma_e}{4}\{J^{f,*}_{x_{i+1/2,j}} + J^{f,n}_{x_{i+1/2,j}}\} = \frac{1}{4}\{E^{f,*}_{x_{i+1/2,j}} + E^{f,n}_{x_{i+1/2,j}}\} \tag{58}$$

**Stage 2**: Along $x$-direction, solve $E_y^{c,n+1}$,$J_y^{c,n+1}$, $K_z^{c,n+1}$, intermediate variable $H_z^{c,**}$ and $E_y^{f,n+1}$,$J_y^{f,n+1}$,$K_z^{f,n+1}$, intermediate variable $H_z^{f,**}$ or $j = 0, 1, \cdots, J_c-1$

(2-a). On coarse sub-domain $\Omega_h^c$ , compute $E_y^{c,n+1}$,$J_y^{c,n+1}$,$K_z^{c,n+1}$ and intermediate variable $H_z^{c,**}$ by

$$\epsilon_0 \frac{E^{c,n+1}_{y_{i,j+1/2}} - E^{c,n}_{y_{i,j+1/2}}}{\Delta t} = -\frac{1}{2}\delta_x^c \{H^{c,**}_{z_{i,j+1/2}} + H^{c,*}_{z_{i,j+1/2}}\} - \frac{1}{2}\{J^{c,n}_{y_{i,j+1/2}} + J^{c,n+1}_{y_{i,j+1/2}}\} \tag{59}$$

$$\mu_0 \frac{H^{c,**}_{z_{i+1/2,j+1/2}} - H^{c,*}_{z_{i+1/2,j+1/2}}}{\Delta t} = -\frac{1}{2}\delta_x^c \{E^{c,n+1}_{y_{i+1/2,j+1/2}} + E^{c,n}_{y_{i+1/2,j+1/2}}\} - \frac{1}{2}\{K^{c,n}_{z_{i+1/2,j+1/2}} + K^{c,n+1}_{z_{i+1/2,j+1/2}}\} \tag{60}$$

$$\gamma_e \frac{J^{c,n+1}_{y_{i,j+1/2}} - J^{c,n}_{y_{i,j+1/2}}}{\Delta t} + \frac{\gamma_e \Gamma_e}{2}\{J^{c,n+1}_{y_{i,j+1/2}} + J^{c,n}_{y_{i,j+1/2}}\} = \frac{1}{2}\{E^{c,n+1}_{y_{i,j+1/2}} + E^{c,n}_{y_{i,j+1/2}}\} \tag{61}$$

$$\gamma_m \frac{K^{c,n+1}_{z_{i+1/2,j+1/2}} - K^{c,n}_{z_{i+1/2,j+1/2}}}{\Delta t} + \frac{\gamma_m \Gamma_m}{2}\{K^{c,n+1}_{z_{i+1/2,j+1/2}} + K^{c,n}_{z_{i+1/2,j+1/2}}\} = \frac{1}{2}\{H^{c,**}_{z_{i+1/2,j+1/2}} + H^{c,*}_{z_{i+1/2,j+1/2}}\} \tag{62}$$

(2-b). On refined sub-domain $\Omega_h^f$ , compute $E_y^{f,n+1}$,$J_y^{f,n+1}$,$K_z^{f,n+1}$ and intermediate variable $H_z^{f,**}$ by

$$\epsilon_0 \frac{E^{f,n+1}_{y_{i,j+1/2}} - E^{f,n}_{y_{i,j+1/2}}}{\Delta t} = -\frac{1}{2}\delta_x^f \{H^{f,**}_{z_{i,j+1/2}} + H^{f,*}_{z_{i,j+1/2}}\} - \frac{1}{2}\{J^{f,n}_{y_{i,j+1/2}} + J^{f,n+1}_{y_{i,j+1/2}}\} \tag{63}$$

$$\mu_0 \frac{H^{f,**}_{z_{i+1/2,j+1/2}} - H^{f,*}_{z_{i+1/2,j+1/2}}}{\Delta t} = -\frac{1}{2}\delta_x^f \{E^{f,n+1}_{y_{i+1/2,j+1/2}} + E^{f,n}_{y_{i+1/2,j+1/2}}\} - \frac{1}{2}\{K^{f,n}_{z_{i+1/2,j+1/2}} + K^{f,n+1}_{z_{i+1/2,j+1/2}}\} \tag{64}$$

$$\gamma_e \frac{J^{f,n+1}_{y_{i,j+1/2}} - J^{f,n}_{y_{i,j+1/2}}}{\Delta t} + \frac{\gamma_e \Gamma_e}{2}\{J^{f,n+1}_{y_{i,j+1/2}} + J^{f,n}_{y_{i,j+1/2}}\} = \frac{1}{2}\{E^{f,n+1}_{y_{i,j+1/2}} + E^{f,n}_{y_{i,j+1/2}}\} \tag{65}$$

$$\gamma_m \frac{K^{f,n+1}_{z_{i+1/2,j+1/2}} - K^{f,n}_{z_{i+1/2,j+1/2}}}{\Delta t} + \frac{\gamma_m \Gamma_m}{2}\{K^{f,n+1}_{z_{i+1/2,j+1/2}} + K^{f,n}_{z_{i+1/2,j+1/2}}\} = \frac{1}{2}\{H^{f,**}_{z_{i+1/2,j+1/2}} + H^{f,*}_{z_{i+1/2,j+1/2}}\} \tag{66}$$

(2-c). On interface $\Gamma$ of $\Omega_h^c$ and $\Omega_h^f$, at $i = I^{int}$, by

$$\begin{aligned}
&-2\epsilon_0\Delta x\delta_t E^{c,n+1/2}_{y_{I^{int},j+1/2}} + \{H^{c,**}_{z_{I^{int}-1/2,j+1/2}} + H^{c,*}_{z_{I^{int}-1/2,j+1/2}}\} - \Delta x(J^{c,n+1}_{y_{I^{int},j+1/2}} + J^{c,n}_{y_{I^{int},j+1/2}}) \\
&\quad = \epsilon_0\Delta x\delta_t E^{f,n+1/2}_{y_{I^{int},2j+1/2}} + \{H^{f,**}_{z_{I^{int}+1/2,2j+1/2}} + H^{f,*}_{z_{I^{int}+1/2,2j+1/2}}\} + \frac{1}{2}\Delta x(J^{f,n+1}_{y_{I^{int},2j+1/2}} + J^{f,n}_{y_{I^{int},2j+1/2}})
\end{aligned} \tag{67}$$

$$E^{c,n+1}_{y_{I^{int},j+1/2}} + E^{c,n}_{y_{I^{int},j+1/2}} = \frac{1}{2}\{E^{f,n+1}_{y_{I^{int},2j+1/2}} + E^{f,n}_{y_{I^{int},2j+1/2}}\} + \frac{1}{2}\{E^{f,n+1}_{y_{I^{int},2j+3/2}} + E^{f,n}_{y_{I^{int},2j+3/2}}\} \tag{68}$$

$$\begin{aligned}
&-2\epsilon_0\Delta x\delta_t E^{c,n+1/2}_{y_{I^{int},j+1/2}} + \{H^{c,**}_{z_{I^{int}-1/2,j+1/2}} + H^{c,*}_{z_{I^{int}-1/2,j+1/2}}\} - \Delta x(J^{c,n+1}_{y_{I^{int},j+1/2}} + J^{c,n}_{y_{I^{int},j+1/2}}) \\
&\quad = \epsilon_0\Delta x\delta_t E^{f,n+1/2}_{y_{I^{int},2j+3/2}} + \{H^{f,**}_{z_{I^{int}+1/2,2j+3/2}} + H^{f,*}_{z_{I^{int}+1/2,2j+3/2}}\} + \frac{1}{2}\Delta x(J^{f,n+1}_{y_{I^{int},2j+3/2}} + J^{f,n}_{y_{I^{int},2j+3/2}})
\end{aligned} \tag{69}$$

**Stage 3**: Along $y$-direction, solve $E_x^{c,n+1}$,$J_x^{c,n+1}$ and $H_z^{c,n+1}$ and $E_x^{f,n+1}$,$J_x^{f,n+1}$ and $H_z^{f,n+1}$.
(3-a). On coarse sub-domain $\Omega_h^c$, compute $E_x^{c,n+1}$,$J_x^{c,n+1}$ and $H_z^{c,n+1}$ for $i = 0, 1, \cdots, I^{int}-1$

$$\epsilon_0\frac{E^{c,n+1}_{x_{i+1/2,j}} - E^{c,*}_{x_{i+1/2,j}}}{\Delta t} = \frac{1}{4}\delta_y^c\{H^{c,n+1}_{z_{i+1/2,j}} + H^{c,**}_{z_{i+1/2,j}}\} - \frac{1}{4}\{J^{c,n+1}_{x_{i+1/2,j}} + J^{c,*}_{x_{i+1/2,j}}\} \tag{70}$$

$$\mu_0\frac{H^{c,n+1}_{z_{i+1/2,j+1/2}} - H^{c,**}_{z_{i+1/2,j+1/2}}}{\Delta t} = \frac{1}{4}\delta_y^c\{E^{c,*}_{x_{i+1/2,j+1/2}} + E^{c,n+1}_{x_{i+1/2,j+1/2}}\} \tag{71}$$

$$\gamma_e\frac{J^{c,n+1}_{x_{i+1/2,j}} - J^{c,*}_{x_{i+1/2,j}}}{\Delta t} + \frac{\gamma_e\Gamma_e}{4}\{J^{c,n+1}_{x_{i+1/2,j}} + J^{c,*}_{x_{i+1/2,j}}\} = \frac{1}{4}\{E^{c,n+1}_{x_{i+1/2,j}} + E^{c,*}_{x_{i+1/2,j}}\} \tag{72}$$

(3-b). On refined sub-domain $\Omega_h^f$, compute $E_x^{f,n+1}$,$J_x^{f,n+1}$ and $H_z^{f,n+1}$ for $i = I^{int}, I^{int}+1, \cdots, I-1$

$$\epsilon_0\frac{E^{f,n+1}_{x_{i+1/2,j}} - E^{f,*}_{x_{i+1/2,j}}}{\Delta t} = \frac{1}{4}\delta_y^f\{H^{f,n+1}_{z_{i+1/2,j}} + H^{f,**}_{z_{i+1/2,j}}\} - \frac{1}{4}\{J^{f,n+1}_{x_{i+1/2,j}} + J^{f,*}_{x_{i+1/2,j}}\} \tag{73}$$

$$\mu_0\frac{H^{f,n+1}_{z_{i+1/2,j+1/2}} - H^{f,**}_{z_{i+1/2,j+1/2}}}{\Delta t} = \frac{1}{4}\delta_y^f\{E^{f,*}_{y_{i+1/2,j+1/2}} + E^{f,n+1}_{y_{i+1/2,j+1/2}}\} \tag{74}$$

$$\gamma_e\frac{J^{f,n+1}_{x_{i+1/2,j}} - J^{f,*}_{x_{i+1/2,j}}}{\Delta t} + \frac{\gamma_e\Gamma_e}{4}\{J^{f,n+1}_{x_{i+1/2,j}} + J^{f,*}_{x_{i+1/2,j}}\} = \frac{1}{4}\{E^{f,*}_{x_{i+1/2,j}} + E^{f,n+1}_{x_{i+1/2,j}}\} \tag{75}$$

And the PEC boundary condition and initial values are provided.

**Remark 1.** *For Stage 2 of GEP-LMR-S-FDTD-II, the fast implementation technique described in Section 3.2 can be utilized. Other two stages, Stage 1 and Stage 3 of GEP-LMR-S-FDTD-II, lead to the tridiagonal systems which can be easily solved by Thomas's algorithm.*

## 5. Numerical experiments

In this section, we will conduct numerical experiments for metamaterial electromagnetic problems to show the global energy conservation and convergence orders of the GEP-LMR-S-FDTD schemes. Let $L^2-$ norm error be

$$Err_{L^2} = (\epsilon_0||E(t_n) - E^n)||^2 + \mu_0||H_z(t_n) - H_z^n||^2 + \gamma_e||J(t_n) - J^n||^2 + \gamma_m||K_z(t_n) - K_z^n||^2)^{\frac{1}{2}}$$

and let the relative error of global energy at time level $n$ be

$$RW^n = \frac{|W^n - W^0|}{|W^0|}$$

Table 1: Errors and temporal convergence orders for Example 1 by the GEP-LMR-S-FDTD schemes with mesh refinement with $\Delta x = \Delta y = \Delta t$ at T =1.

| | $\Delta t$ | $err_{L^2}$ | $Order$ |
|---|---|---|---|
| GEP-LMR-S-FDTD-I | 1/20 | 4.138e-2 | |
| | 1/40 | 2.052e-2 | 1.0117 |
| | 1/80 | 1.023e-2 | 1.0081 |
| | 1/160 | 5.108e-3 | 1.0061 |
| GEP-LMR-S-FDTD-II | 1/20 | 2.124e-3 | |
| | 1/40 | 5.25e-4 | 2.0178 |
| | 1/80 | 1.30e-4 | 2.0088 |
| | 1/160 | 3.25e-5 | 2.0043 |
| | 1/320 | 8.11e-6 | 2.0021 |

where $W^n$ is the discrete global energy at time level $n$ over the domain of coarse and fine meshes.

**Example 1.** Consider Maxwell's equations with Drude model over domain $\Omega = [0,1] \times [0,1]$ and with PEC boundary condition on $\partial\Omega$. The exact solution of the problem is considered as

$$E_x(x,y,t) = (\frac{1}{\omega^2\pi} - \frac{1}{\omega})\cos(k_x\pi x)\sin(k_y\pi y)e^{-\omega\pi t},\ E_y(x,y,t) = -(\frac{1}{\omega^2\pi} - \frac{1}{\omega})\sin(k_x\pi x)\cos(k_y\pi y)e^{-\omega\pi t},$$
$$H_z(x,y,t) = (\frac{1}{\omega\pi} - 1)\cos(k_x\pi x)\cos(k_y\pi y)e^{-\omega\pi t},\ K_z(x,y,t) = \cos(k_x\pi x)\cos(k_y\pi y)e^{-\omega\pi t}$$
$$J_x(x,y,t) = \frac{1}{\omega}\cos(k_x\pi x)\sin(k_y\pi y)e^{-\omega\pi t},\ J_y(x,y,t) = -\frac{1}{\omega}\sin(k_x\pi x)\cos(k_y\pi y)e^{-\omega\pi t},$$

with parameters $\epsilon_0 = \mu_0 = 1$, $\gamma_e = \gamma_m = 1$, $\Gamma_e = \Gamma_m = 1$, $k_x = k_y = 1$, $\omega = \sqrt{k_x^2 + k_y^2}$, and the right side functions and initial values are given by the exact solution.

Table 2: Errors and space convergence orders for Example 1 by the GEP-LMR-S-FDTD schemes with mesh refinement at $T = 1$.

| | $\Delta x = \Delta y$ | $err_{L^2}$ | $Order$ |
|---|---|---|---|
| GEP-LMR-S-FDTD-I | 1/20 | 1.88e-03 | |
| (with $\Delta t = \Delta x^2$) | 1/40 | 4.67e-04 | 2.005 |
| | 1/60 | 2.07e-04 | 2.004 |
| | 1/80 | 1.17e-04 | 2.003 |
| GEP-LMR-S-FDTD-II | 1/20 | 2.124e-3 | |
| (with $\Delta t = \Delta x$) | 1/40 | 5.25e-4 | 2.0178 |
| | 1/80 | 1.30e-4 | 2.0088 |
| | 1/160 | 3.25e-5 | 2.0043 |
| | 1/320 | 8.11e-6 | 2.0021 |

Numerical solutions by the GEC-LMR-S-FDTD I and II schemes are computed to test their global energy conservations and their convergence rates in time and space. The domain $\Omega$ is divided into $\Omega_1$ and $\Omega_2$, where $\Omega_1 = [0, 0.5] \times [0, 1]$ and $\Omega_2 = [0.5, 1] \times [0, 1]$. $\Omega_1$ is meshed by coarse step sizes $2\Delta x$ and $2\Delta y$ and $\Omega_2$ is meshed by fine fine step sizes $\Delta x$ and $\Delta y$. Table 1 shows the errors and time convergence orders of the two schemes with different time step sizes. It clearly shows the convergence order of GEP-LMR-FDTD-I is first order and the convergence order of GEP-LMR-FDTD-II is second order. Table 2 shows the errors

Table 3: Relative errors of global energy and computational time for the GEP-LMR-S-FDTD-I implementations with mesh refinement and with $\Delta t = \Delta x = \Delta y$ at different time.

| Scheme | Mesh (h) | | | | |
|---|---|---|---|---|---|
| | | 1/80 | 1/160 | 1/320 | 1/640 |
| FI-GEP-LMR-S-FDTD-I | ReErr | 1.98e-14 | 2.44e-14 | 3.46e-14 | 1.64e-14 |
| | CPU time (s) | 1.154308 | 7.897727 | 35.249692 | 173.543342 |
| GEP-LMR-S-FDTD-I | ReErr | 1.954e-14 | 2.42e-14 | 3.44e-14 | 1.53e-14 |
| | CPU time (s) | 1.337623 | 9.755095 | 108.697241 | 3047.183608 |

Table 4: Relative errors of global energy and computational time for the GEP-LMR-S-FDTD-II implementations with mesh refinement and with $\Delta t = \Delta x = \Delta y$ at different time.

| Scheme | Mesh (h) | | | | |
|---|---|---|---|---|---|
| | | 1/80 | 1/160 | 1/320 | 1/640 |
| FI-GEP-LMR-S-FDTD-II | ReErr | 1.33e-15 | 3.15e-14 | 3.89e-15 | 1.05e-14 |
| | CPU time (s) | 1.410889 | 7.209083 | 37.172014 | 280.623585 |
| GEP-LMR-S-FDTD-II | ReErr | 1.33e-15 | 3.18e-14 | 4.00e-15 | 3.95e-14 |
| | CPU time (s) | 1.557713 | 10.511077 | 118.201917 | 2746.853513 |

and space convergence orders of the two schemes with different space step sizes. It can be clearly seen that the space orders of convergence of both GEP-LMR-S-FDTD-I and GEP-LMR-S-FDTD-II are second order. Table 5 shows the relative errors of global energy at different time, where the problem is with initial values and without right side functions. The errors reach $10^{-13}$ which clearly shows the two schemes of GEP-LMR-S-FDTD are global energy preserving.

Table 3 compares CPU time of fast implementation algorithm and normal implementation. When the spatial size h decreases the CPU time spent on fast algorithm and normal algorithm varies dramatically. It shows that fast algorithm of GEP-LMR-S-FDTD-I takes less CPU time than the normal algorithm. For example, when h = $\frac{1}{640}$ the fast algorithm takes 173 seconds to get the result while the normal algorithm takes 3047 seconds.

Table 4 illustrates the CPU time of fast implementation algorithm on GEP-LMR-S-FDTD-II. Since the fast algorithm was implemented in the 2nd stage. We can clearly see the fast methods takes less CPU time than normal algorithm. For example, when h = $\frac{1}{640}$ the fast algorithm takes 280.623585 seconds to get the result while the normal algorithm takes 2746.853513 seconds.

The code is available at `https://github.com/Cwang422/GEP-LMR-S-FDTD`. Table 3 and Table 4 are generated by Intel(R) Core(TM) i3-1000NG4 CPU @ 1.10GHz.

Table 5: Relative errors of global energy for Example 1 by the GEP-LMR-S-FDTD schemes with mesh refinement and with $\Delta t = \Delta x = \Delta y = 1/160$ at different time.

| t | GEP-LMR-S-FDTD-I | GEP-LMR-S-FDTD-II |
|---|---|---|
| 2 | 2.00975e-14 | 5.70654e-14 |
| 4 | 3.73034e-14 | 8.84847e-14 |
| 6 | 5.08482e-14 | 1.07691e-13 |
| 8 | 6.25055e-14 | 1.19904e-13 |
| 10 | 7.36077e-14 | 1.27009e-13 |

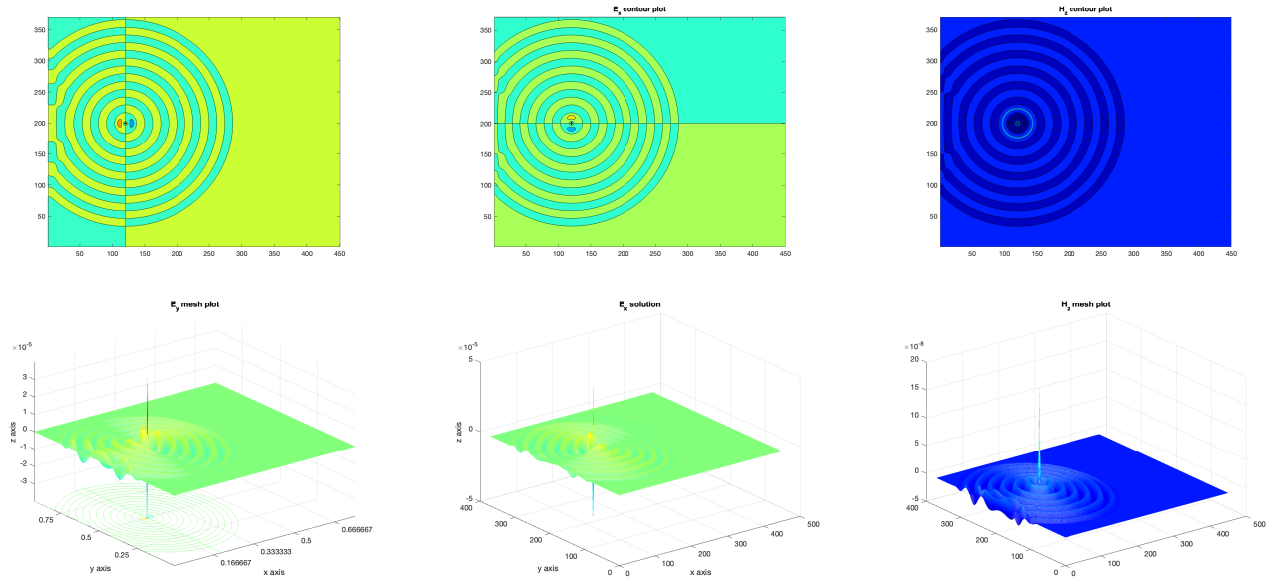

Figure 3: Numerical solutions of $E_y$, $E_x$ and $H_z$ by GEP-LMR-S-FDTD scheme at $t = 500\Delta t$.

**Example 2.** In this example, we simulate the electromagnetic propagation in vacuum and with sinusoidal point source. The domain is $\Omega = [0, 450h]\times[0, 370h]$, where $h = 1/5000m$. We implement PEC boundary condition for the problem. Take $\Delta t{=}\frac{C_N h}{\sqrt{2}c_0}$ with $c_0 = 3\times 10^8 m/s$ and $C_N = 0.5$. Interface between coarse and fine meshes is located at $x = 225h$. The step size for the left coarse mesh part is $2h$ while the fine step size for the right fine mesh part is $h$. The parameters are $\mu_0 = 4\pi \times 10^{-7} H/m$ and $\epsilon_0 = 8.85 \times 10^{-12} F/m$, respectively. The point source is located at $(100h, 200h)$ with

$$f(t) = \begin{cases} 0 & t \le 0 \\ g_1(t)\sin(\omega_0 t) & 0 \le t \le mT_p \\ \sin(\omega_0 t) & mT_p \le t \le (m+k)T_p \\ g_2(t)\sin(\omega_0 t) & (m+k)T_p \le t \le (2m+k)T_p \\ 0 & t \ge (2m+k)T_p \end{cases}$$

where $f_0 = 30GH_z$, $\omega_0 = 2\pi f_0$, $T_p = \frac{1}{f_0}$, $m = 2$ , $k = 100$, and

$$g_1(t) = 10\rho_1^3 - 15\rho_1^4 + 6\rho_1^5, \rho_1 = \frac{t}{mT_p}; \quad g_2(t) = 10\rho_2^3 - 15\rho_2^4 + 6\rho_2^5, \rho_2 = t - \frac{(m+k)T_p}{mT_p}.$$

Numerical solutions of $E_y, E_x$ and $H_z$ by GEP-LMR-S-FDTD are showed at $t = 360\Delta t$ in Fig. 3. As we can see from the figures the electromagnetic wave has reached both interface and PEC boundary. The mesh refinement at interface does not affect the propagation across the interface between coarse and fine meshes. However, the PEC boundary affects its propagation on the left boundary.

Numerical distributions of magnetic filed $H_z$ at different time $t = 300\Delta t, 360\Delta t$ and $500\Delta t$ are depicted in Fig. 4. The magnetic field moves away from the excitation source. The source is exited in the coarse sub-domain and the wave gradually spreads to refined sub-domain, crossing the interface between coarse and fine meshes and meeting PEC boundary.

**Example 3.** We consider Maxwell's equations with initial waves and PEC boundary. The domain of simulation is $\Omega = [0, 16\mu m] \times [0, 5.4\mu m]$. The permeability and permittivity

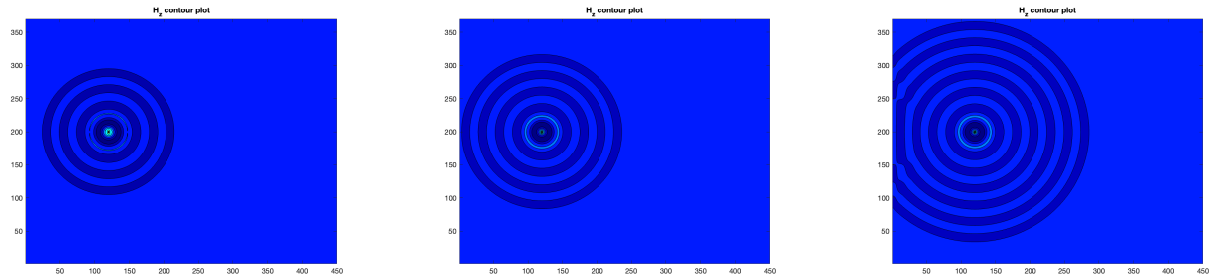

Figure 4: Numerical distributions of $H_z$ by GEP-LMR-S-FDTD scheme at different time $t = 300\Delta t, 360\Delta t$ and $500\Delta t$.

are given by $\epsilon_0 = 1$ and $\mu_0 = 1$, respectively. The magnetic field is initialized with a Gaussian pulse as

$$H_z(x, y, 0) = \exp(-((x - x_0)^2 + (y - y_0)^2)/\sigma^2)$$

with $\sigma = 0.40\mu m$, $x_0 = 6\mu m$ and $y_0 = 2.70\mu m$, and $E_y(x, y, 0) = H_z(x, y, 0)$, $E_x(x, y, 0) = 0$. The interface of coarse and fine meshes is located at $x = 8\mu m$. The interface of coarse and fine meshes is located at $x = 8\mu m$. Coarse step size for the left sub-domain is $2h$ and fine step size for the right sub-domain is $h$ by taking $h = \frac{1}{25}\mu m$ and $\Delta t = \frac{h}{\sqrt{2}}$.

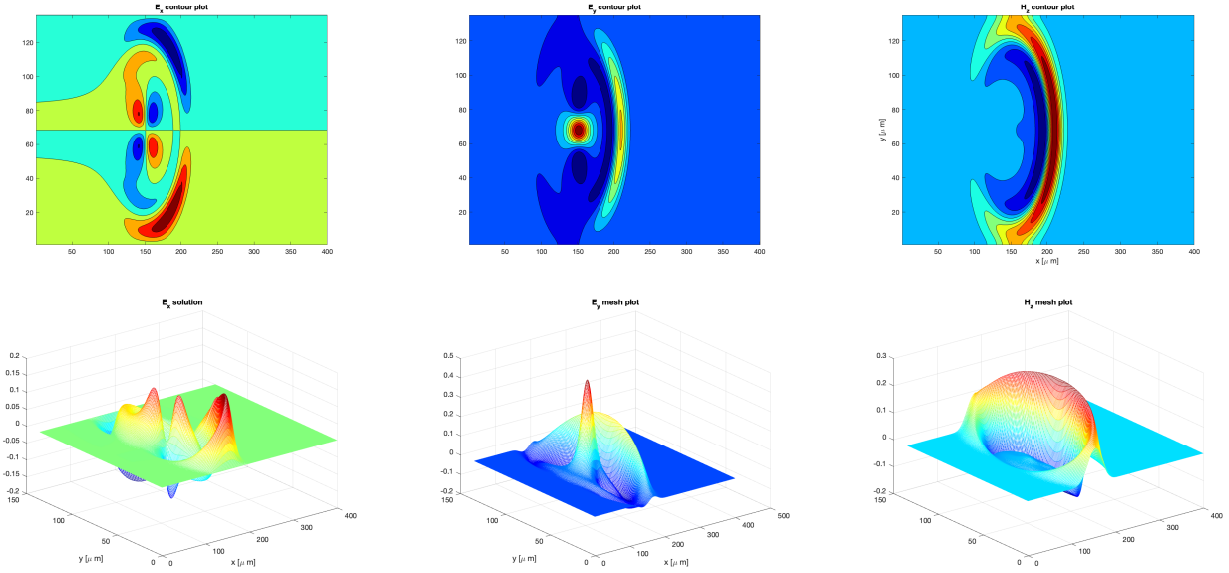

Figure 5: Numerical solutions of $E_x$, $E_y$ and $H_z$ by GEP-LMR-S-FDTD at $t = 80\Delta t$.

Fig. 5 shows the electromagnetic waves of $E_x$,$E_y$ and $H_z$ by GEP-LMR-S-FDTD scheme at time $t = 80\Delta t$, which have crossed the interface from coarse sub-domain to refined sub-domain. The refinement at interface does not affect the propagation of the electromagnetic waves.

The electromagnetic wave propagates from left to right. Fig. 6 shows the wave $H_z$ moves outward from coarse sub-domain to refined sub-domain at different time $t = 0, 50\Delta t, 80\Delta t$ and $120\Delta t$. The wave is not affected by the refinement at interface, but the wave is reflected from the PEC boundary.

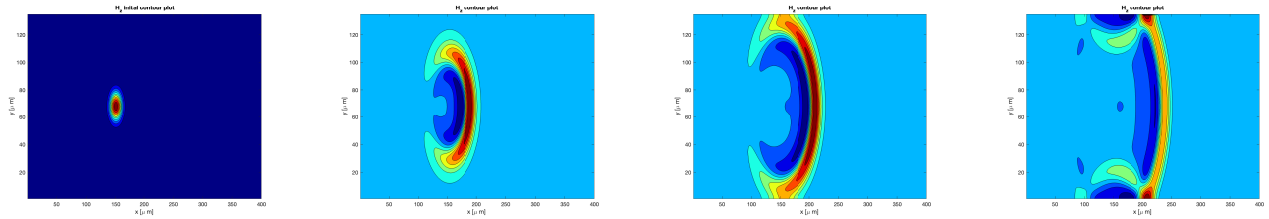

Figure 6: Contour plots of numerical magnetic field $H_z$ by GEP-LMR-S-FDTD scheme at different time $t = 0, 50\Delta t, 80\Delta t$ and $120\Delta t$.

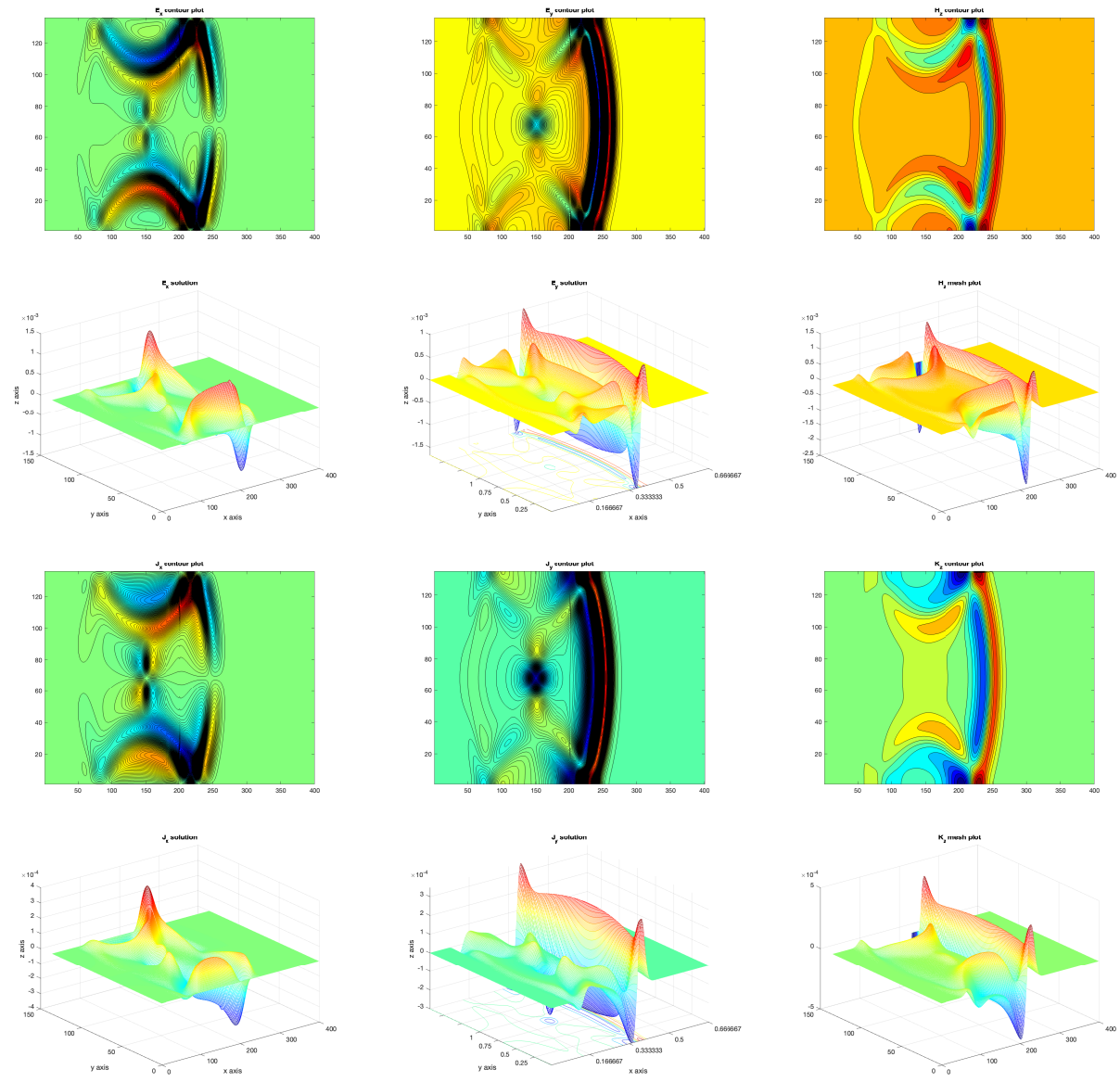

Figure 7: Numerical distributions of $H_z$, $E_x$, $E_y$ and $J_x$, $J_y$, $K_z$ by GEP-LMR-S-FDTD scheme at $t = 290\Delta t$.

**Example 4.** In this example, we consider electromagnetic propagation within Drude metamaterials due to initial magnetic wave. The permeability and permittivity are given by $\epsilon_0 = 1$, $\mu_0 = 1$, $\gamma_e = \gamma_m = 1$ and $\Gamma_e = \Gamma_m = 1$, respectively. The domain is $\Omega = [0, 16\mu m] \times [0, 5.4\mu m]$ and the PEC boundary condition is provided. The initial Gaussian

pulse is applied as

$$H_z(x, y, 0) = \exp([-((x - x_0)^2 + (y - y_0)^2)/\sigma^2])$$

with $\sigma = 0.40\ \mu m$, $x_0 = 6\ \mu m$,$y_0 = 2.70\ \mu m$, and $E_y(x, y, 0) = H_z(x, y, 0)$, $E_x(x, y, 0) = 0$, $J_x(x, y, 0) = 0$, $J_y(x, y, 0) = 0$, $K_z(x, y, 0) = 0$. We divide the domain into two sub-domains at the interface between coarse and refined meshes is located at $x = 8\mu m$. Coarse step size for the left sub-domain is $2h$ and fine step size for the right sub-domain is $h$. Take $h = \frac{1}{25}\mu m$ and $\Delta t = \frac{h}{\sqrt{2}}$.

The initial Gaussian pulse is exited in the left coarse sub-domain and the electromagnetic wave then moves right fine sub-domain as time goes. Fig. 7 shows the numerical distributions of electromagnetic waves of $H_z$, $E_x$, $E_y$ and $J_x$, $J_y$, $K_z$ at time $t = 290\Delta t$. The propagation of electromagnetic waves in Drude metamaterials does not affect by the interface of coarse and refined meshes while it is clearly affected by PEC boundary.

**Example 5.** We now consider the DNG (double negative material) models excited by a point source. The considered domain is $\Omega = [0, 450h] \times [0, 370h]$ where it contains a DNG region $[225h, 450h] \times [0, 370h]$. The interface of coarse and fine meshes is located at $x = 225h$. The point source is imposed to the $H_z$ component and its temporal form is set to be the $m - n - m$ cycle function with the same parameters as Example 2. The point source is located at $(180h, 170h)$, which is same as the one in Example 2. $\epsilon_0 = 8.85 \times 10^{-12} F/m$, $\mu_0 = 4\pi \times 10^{-7} H/m$, $\Gamma_e = \Gamma_m = 1 \times 10^8 s^{-1}$, $f_0 = 30GH_z$, $\omega_0 = 2\pi f_0$ and $\omega_{pe} = \omega_{pm} = \sqrt{2}\omega_0$ or $\sqrt{7}\omega_0$.

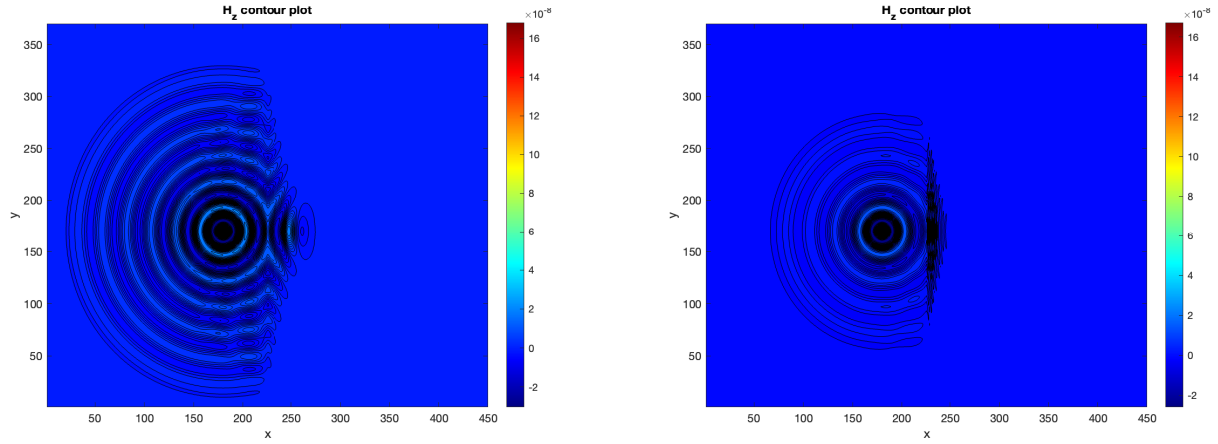


Figure 8: Numerical distribution of $H_z$ by GEP-LMR-S-FDTD scheme for the Drude model with $n_r = -1$ (left) and with $n_r = -6$ (right).

We compute the electromagnetic waves excited by the sinusoidal point source in the domain containing both vacuum and DNG media with negative refractive index $n_r = -1$ or $n_r = -6$. Fig. 8 plots the numerical magnetic field $H_z$. It depicts the intensities at the time $T = 1000\Delta t$. We can see the inverse reflection when the magnetic waves enter into the DNG region compared with the case in vacuum.

## Acknowledgments

This work is supported by Natural Sciences and Engineering Research Council of Canada.

## References


[1] F. Bilotti and L.Sevgi, Metamaterials: Definitions, properties, applications, and FDTD-based modeling and simulation, Int. J. RF Microw. Comput. Eng., 22 (2012), 421-421.

[2] Engheta, N., Ziolkowski, R. :A positive future for double-negative metamaterials, IEEE Trans. Microw. Theor. Tech., 53 (2005), 1535-1556.

[3] Holden,A.J.:Towards some real applications for negative materials, Photonic Nanostruct. Fundam. Appl., 3 (2005), 96-99.

[4] R. A. Shelby, D. R. Smith, and S. Schultz, Experimental verification of a negative index of refraction, Science, 292 (2001), 77-79.

[5] M. K. Kärkkäinen, Numerical study of wave propagation in uniaxially anisotropic Lorentzian backward-wave slab, Phys. Rev. E, 68 (2003), 026602.

[6] Y. Hao and R. Mittra, FDTD modeling of metamaterials: Theory and applications, Artech House, 2008.

[7] V. A. Bokil and N. L. Gibson, Analysis of spatial high-order finite difference methods for Maxwell's equations in dispersive media., IMA J. Numer. Anal., 32 (2012), 926-956.

[8] H. Wang, B. Wu, Z. Huang, et al., A symplectic FDTD algorithm for the simulations of lossy dispersive materials, Comput. Phys. Comm., 185 (2014), 862-872.

[9] D. R. Gibbins, C. J. Railton, I. J. Craddock, et al., A numerical study of Debye and conductive dispersion in high-dielectric materials using a general ADE-FDTD algorithm, IEEE Trans. Antennas and Propagation, 64 (2016), 2401-2409.

[10] G. Cevini, G. Oliveri and M. Raffetto, Further comments on the performances of finite element simulators for the solution of electromagnetic problems involving metamaterials, Microw. Opt. Technol. Lett., 48 (2006), 2524-2529.

[11] S. Lanteri and C. Scheid, Convergence of a discontinuous Galerkin scheme for the mixed time-domain Maxwell's equations in dispersive media, IMA J. Numer. Anal., 33 (2013), 432-459.

[12] J. Li, Y. Huang and W. Yang, Numerical study of the plasma-Lorentz model in metamaterials, J. Sci. Comput., 54 (2013), 121-144.

[13] K. Li, T. Huang, L. Li, et al., A reduced-order DG formulation based on POD method for the time-domain Maxwell's equations in dispersive media, J. Comput. Appl. Math., 336 (2018), 249-266.

[14] C. Shi, J. Li and C.-W. Shu, Discontinuous Galerkin methods for Maxwell's equations in Drude metamaterials on unstructured meshes, J. Comput. Appl. Math., 342 (2018), 147-163.

[15] K. Yee, Numerical solution of initial boundary value problems involving Maxwell's equations in isotropic media, IEEE Trans. Antenn. Propag.,14 (1966), 302-307.

[16] A. Taflove and S. Hagness, Computational electrodynamics: the finite-difference time-domain method. Artech House, Boston, 2000.

[17] A. Pekmezci, E. Topuz and L. Sevgi, Finite difference time domain formulation for epsilon-negative medium using wave equation, Int. J. RF Microw. Compt. Aid. Eng., 26 (2016), 304-310.

[18] D. Zhang, I. Capoglu, Y. Li, et al., Finite-difference time-domain-based optical microscopy simulation of dispersive media facilitates the development of optical imaging techniques, J. Biomed. Opt., 21 (2016), 065004.

[19] N. V. Kantartzis and T. D. Tsiboukis, Rigorous ADI-FDTD Analysis of Left-Handed Metamaterials in Optimally-Designed EMC Applications, Int. J. Comput. Math. Elect. Elect. Eng., 25 (2006), 677-690.

[20] X. Wang, J. Gao, Z. Chen, et al., Unconditionally stable one-step leapfrog ADI-FDTD for dispersive media, IEEE Trans. Antennas and Propagation, 67 (2019), 2829-2834.

[21] E. K. Kim, S. A. Ha, J. Lee, et al., Three-dimensional efficient dispersive alternating-direction-implicit finite-difference time-domain algorithm using a quadratic complex rational function, Opt. Express, 23 (2015), 873-881.

[22] V. E. Nascimento, K. Y. Jung, B. V. Borges, et al., A study on unconditionally stable FDTD methods for the modeling of metamaterials, J. Lightwave Technol., 27 (2009), 4241-4249.

[23] W. Li and D. Liang, Symmetric energy-conserved S-FDTD scheme for two-dimensional Maxwell's equations in negative index metamaterials, J. Sci. Comput., 69 (2016), 696-735.

[24] W. Li and D. Liang, The Energy Conservative Splitting FDTD scheme and its Energy Identities for Metamaterial Electromagnetic Lorentz System, Comput. Phys. Commun., 239 (2019), 94-111.

[25] I. S. Kim and W.J.R. Hoefer, A local mesh refinement algorithm for the time domain-finite difference method using Maxwell's curl equations, IEEE Trans. Microw. Theory Tech., 38 (1990), 812-815.

[26] A. R. Zakharian, M. Brio and J. V. Moloney, FDTD based second-order accurate local mesh refinement method for Maxwell's equations in two space dimensions, Commun. Math. Sci., 2 (2004), 497-513.

[27] Z. Chen and I. Ahmed, A hybrid ADI-FDTD scheme and its comparisons with the FDTD method, Digests of Int. Symp on Ant. Prop., 4 (2003), 360-263.

[28] F. Collino, T. Fouquet and P. Joly, A conservative space-time mesh refinement method for the 1-D wave equation. Part I: construction, Numer. Math., 95 (2003), 197-221.

[29] P. Joly and J. Rodriguez, An error analysis of conservative space-time mesh refinement methods for the one-dimensional wave equation, SIAM J. Numer. Anal., 43 (2005), 825-859.

[30] J. Xie, D. Liang and Z. Zhang, Energy-preserving local mesh-refined splitting FDTD schemes for two dimensional Maxwell's equations, J. Comput. Phys., 425 (2021), 109896.

[31] V. G. Veselago, L. Braginsky, V. Shklover, et al., Negative Refractive Index Materials, J. Comput. Theor. Nanosci., 3 (2006), 1-30.

[32] T. Cui and J. Kong, Time-domain electromagnetic energy in a frequency-dispersive left-handed medium, Phys. Rev. B, 70 (2004), 205106.

[33] J. Li and A. Wood, Finite element analysis for wave propagation in double negative metamaterials, J. Sci. Comput., 32 (2007), 263-286.

[34] R. Ruppin, Electromagnetic energy density in a dispersive and absorptive material, Phys. Lett. A , 299 (2002), 309-312.